

Technical note: Impact of beam properties for uveal melanoma proton therapy—An in silico planning study

Jörg Wulff^{1,2,3} | Benjamin Koska^{1,2,3} | Martin Janson⁴ | Christian Bäumer^{1,2,3,5,6} |
 Andrea Denker^{7,8} | Dirk Geismar^{1,2,3,9} | Johannes Gollrad¹⁰ |
 Beate Timmermann^{1,2,3,5,9} | Jens Heufelder^{11,12}

¹West German Proton Therapy Centre Essen (WPE), Essen, Germany

²University Hospital Essen, Essen, Germany

³West German Cancer Centre (WTZ), Essen, Germany

⁴RaySearch Laboratories, Stockholm, Sweden

⁵German Cancer Consortium (DKTK), Heidelberg, Germany

⁶TU Dortmund University, Dortmund, Germany

⁷Helmholtz-Zentrum Berlin für Materialien und Energie, Protonentherapie, Germany

⁸Beuth-Hochschule für Technik, Berlin, Germany

⁹Department of Particle Therapy, Essen, Germany

¹⁰Charité—Universitätsmedizin Berlin, Department of Radiation Oncology and Radiotherapy, Berlin, Germany

¹¹Charité—Universitätsmedizin Berlin, Department of Ophthalmology, Berlin, Germany

¹²Charité—Universitätsmedizin Berlin, BerlinProtonen am Helmholtz-Zentrum für Materialien und Energie, Berlin, Germany

Correspondence

Jörg Wulff, Westdeutsches Protonentherapiezentrum Essen (WPE) gGmbH, Am Mühlenbach 1, 45147 Essen, Germany.
 Email: joerg.wulff@uk-essen.de

Abstract

Purpose: To evaluate the impact of beam quality in terms of distal fall-off (DFO, 90%–10%) and lateral penumbra (LP, 80%–20%) of single beam ocular proton therapy (OPT) and to derive resulting ideal requirements for future systems.

Methods: Nine different beam models with DFO varying between 1 and 4 mm and LP between 1 and 4 mm were created. Beam models were incorporated into the RayStation with RayOcular treatment planning system version 10 B (RaySearch Laboratories, Stockholm, Sweden). Each beam model was applied for eight typical clinical cases, covering different sizes and locations of uveal melanoma. Plans with and without an additional wedge were created, resulting in 117 plans with a total prescribed median dose of 60 Gy(RBE) to the clinical target volume. Treatment plans were analyzed in terms of V20–V80 penumbra volume, D1 (dose to 1% of the volume) for optic disc and macula, optic nerve V30 (volume receiving 30 Gy(RBE), i.e., 50% of prescription), as well as average dose to lens and ciliary body. An LP-dependent aperture margin was based on estimated uncertainties, ranging from 1.7 to 4.0 mm.

Results: V20–V80 showed a strong influence by LP, while DFO was less relevant. The optic disc D1 reached an extra dose of up to 3000 cGy(RBE), comparing the defined technical limit of DFO = LP = 1 mm with DFO = 3 mm/LP = 4 mm. The latter may result from a pencil-beam scanning (PBS) system with static apertures. Plans employing a wedge showed an improvement for organs at risk sparing.

Conclusion: Plan quality is strongly influenced by initial beam parameters. The impact of LP is more pronounced when compared to DFO. The latter becomes important in the treatment of posterior tumors near the macula, optic disc or optic nerve. The plan quality achieved by dedicated OPT nozzles in single- or double-scattering design might not be achievable with modified PBS systems.

KEYWORDS

distal fall-off, lateral penumbra, proton therapy, uveal melanoma

This is an open access article under the terms of the [Creative Commons Attribution](https://creativecommons.org/licenses/by/4.0/) License, which permits use, distribution and reproduction in any medium, provided the original work is properly cited.

© 2022 The Authors. *Medical Physics* published by Wiley Periodicals LLC on behalf of American Association of Physicists in Medicine.

1 | INTRODUCTION

Proton therapy (PT) has been used for treatment of uveal melanoma for decades dating back to the 1970s when Massachusetts General Hospital started its first experiments.¹ About 30 000 patients have been treated with tumor control rates of 95% or above.^{2–5} The efficacy of PT for uveal melanoma is now widely accepted making it attractive for larger multi-room PT centers to establish specific eye treatment programs. The quality of the proton treatment, specifically in terms of sparing organs at risk (OARs), is directly depending on the beam properties. The dose distribution of a laterally collimated broad beam spread-out Bragg-peak (SOBP) is typically characterized in terms of lateral penumbra (LP) and distal fall-off (DFO). Those two parameters depend on the accelerator and beam delivery technique used and may both vary between 1 and 3 mm for dedicated eye treatment nozzles.^{6–8} The lateral spreading of the proton beam is typically achieved by a single- or double-scattering systems. The pencil-beam scanning (PBS) technique with apertures can in principle be applied as well.^{9–11}

The DFO of a generated SOBP is impacted by the energy spread at the treatment nozzle exit. Here a balance between high dose rate, maximum field size, and energy spread needs to be defined. The pioneering research centers offering PT were mainly equipped with cyclotrons providing energies of about 60–75 MeV (i.e., water-equivalent ranges of 30–40 mm), requiring only little degradation to adjust range to target depth. Additionally, these machines provide a sufficiently high dose rate.^{8,12} In contrast, multi-room facilities equipped with high-energy cyclotrons, need a substantially larger energy degradation, which affects the treatment beam energy spread and thus the DFO. A too strict energy filtering directly behind the energy degrader in an energy selection system results in low transmission, that is, high dose rate losses. Generally, a higher energy allows beam transport to the nozzle with a higher dose rate. It then however requires further energy degradation within the nozzle by means of a degrader/energy absorber, which introduces an energy spread. No further energy filtering in the nozzle is possible, leading to a higher DFO than in case of energy reduction behind the cyclotron.⁶

Centers equipped with a synchrotron have an intrinsically narrow energy band for selected energies with a corresponding small DFO and LP, though lower dose rates as compared to the cyclotron-based systems.¹¹ In general, the DFO and LP vary considerably between ocular PT centers.⁶

Although the benefit of a sharp LP/DFO is obvious in order to protect neighboring OARs, it is not clear how this exactly translates into plan quality. In a recent interinstitutional comparison it was concluded that clinical outcomes are highly dependent on the centers' beam properties.⁷ Weber et al.¹³ compared different radio-

therapy modalities and showed the general benefit of ocular PT with a dedicated scattering nozzle. However, the modeling accuracy of the Paul-Scherrer Institute (PSI) OPTIS system in this planning study was limited as the beam model was simplified by neglecting collimation. There is a general lack of systematic comparison in terms of treatment quality for different combinations of LP and DFO as they result from technical implementation of PT. It is thus per se not clear which parameter has a larger clinical relevance and thus could be a clinical requirement driving future proton system designs, such as combinations of PBS with aperture.

The impact of beam properties depends on the target margin applied in planning. The *distal/proximal* margin is commonly applied in proton ocular treatments with 2.5 mm and considers uncertainties in absolute range accuracy and reproducibility, setup uncertainties and uncertainties in the assignment of densities/relative stopping powers in the eye model. The commonly applied *lateral* aperture margin is 2.0–2.5 mm, mostly irrespective of the LP. It represents uncertainties in the patient setup, eye model as well as delivery uncertainties and a possible microscopic tumor spread.^{4,6,8,14–18} The exact construction of those margins is not always clearly described, but is directly linked to the expected uncertainties.

The present study aimed at a systematic in silico plan comparison using clinical uveal melanoma cases treated prior to this study with protons by testing different combinations of LP and DFO. In this way it was possible to investigate the relevance of LP and/or DFO on plan quality in terms of dose to OARs. Treatment plans were created within the RayStation (RaySearch Laboratories, Stockholm, Sweden) module RayOcular. Lateral target margins were deduced for the different combinations of LP and DFO, following an analysis of involved uncertainties.

2 | METHODS

2.1 | RayOcular

The RayStation 10B treatment planning system (TPS) was used for a plan intercomparison. RayOcular is a module within the RayStation system, which allows a model-based approach comparable to the EYEPLAN and OCTOPUS planning systems.^{1,8,19,20} The eye and tumor models in RayOcular can be based on funduscopy images and other ophthalmological data, as well as on volumetric computed tomography (CT) and magnetic resonance imaging (MRI) information. The general workflow of clip-based, variable eye gaze angle planning¹ is supported. All calculations were performed with the currently available pencil-beam algorithm on a 0.2 mm dose-grid.

2.2 | In silico modeling of proton distributions using RayOcular

To study the effect of the magnitude of LP (80%–20%) and DFO (90%–10%) on plan quality (defined in Section 2.5), nine beam models with different combinations of LP and DFO were prepared. The models were created to give a nearly constant LP and DFO for various ranges (*R*) and modulation widths (*M*) of the fields. Note, variations with depth are caused by physical process of scattering modeled by the pencil-beam algorithm. The LP was defined at a depth corresponding to the middle of the SOBPs, with the phantom surface positioned 2 cm upstream of the isocenter and with a 5 cm air-gap between phantom and aperture. Thus, a system with 7 cm distance between aperture and isocenter was modeled, representing a typical Ocular PT fixed beam nozzle design.^{6,7} The positioning of the phantom surface 2 cm upstream of isocenter was chosen to mimic a typical depth of an ocular melanoma in the posterior part of the eye. The *R*s of the models can be selected continuously, while *M*s are supported in steps of 3 mm, reflecting commonly available systems.⁷ Table 1 summarizes the models used in this study.

The values in Table 1 were chosen to represent possible beam qualities used in ocular PT^{6–9,21,22} with DFO and LPs ranging from 1 to 4 mm. Model #1 was considered as the technical lower limit, while model #9 on the other hand represents a combination, that may result from a cyclotron-based PBS system with a static aperture.

2.3 | Clinical cases

Eight clinical cases were investigated with varying tumor size and location. The clinical cases

TABLE 1 Overview of the nine beam-model properties used within the plan comparison

Model ID #	DFO (90%–10%) (mm)	LP (80%–20%) (mm)
1	1	1
2	2	1
3	3	1
4	4	1
5	1	2
6	2	2
7	3	2
8	4	2
9	3	4

Note: The lateral penumbra is defined at middle of all available spread-out Bragg-peaks (SOBPs) (in total 45 per model) with the phantom surface 2 cm upstream of the isocenter and with a 5 cm airgap between phantom and aperture.

Abbreviations: DFO, distal fall-off; LP, lateral penumbra.

were based on data from patients of the Charité—Universitätsmedizin Berlin previously treated with protons at the Helmholtz-Zentrum Berlin für Materialien und Energie (HZB). Eye and tumor modeling was performed on CT and MRI information and/or fundus imaging. Optical coherence tomography, ultrasound imaging, and ocular biometry served as additional source of information for defining tumor size, distance between tumor and optic disc/macula, and eye lengths, respectively.

For OARs the default dimensions of the RayOcular model were used. The macula was considered as a cylinder within the sclera with 1.5 mm diameter and 0.4 mm height and being attached to the outer surface of the retina. The optic disc was modeled as a cylinder within the retina with 1.5 mm diameter and 0.4 mm height. The optic nerve was modeled as a cylinder starting within the sclera with 1.5 mm diameter and length of 10 mm and being attached to the optic disc. The pitch/yaw angle of the optic nerve relative to the surface of the eye model was adjusted, based on the CT/MRI information. The skin plane position, that is, the distance between the most anterior part of the cornea and the plane defining the surrounding of the eye model, was taken from the clinical measurements and varied between 3 mm and 10 mm, depending on the tumor location and fixation angle.

In all cases a gross tumor volume (GTV)²³ was defined based on the available data and ranged between 51.6 and 657.4 mm³. The possible microscopic extension was not considered in a separate clinical target volume (CTV), that is, CTV was set equal to GTV, which is a common approach in ocular proton therapy (OPTs).

Figure 1 exemplarily displays dose planes for all treatment plans using model DFO = 1 mm/LP = 1 mm. The dose distributions were normalized to a median dose of 60 Gy(RBE) as prescribed in four fractions. Note, the dose volume in the selected slice may appear larger than necessary, caused by the fact that the distal range was adapted to sufficiently cover the most distal part of the CTV along the beam direction. Figure 1 also illustrates the 50% isodose from model #9 exemplarily for case #1.

A wedge made of polymethylmethacrylat (PMMA) with angles between 30° and 60° was employed in plans except #1, 2, 5 to limit the dose to the optic disc/macula by reducing the distal range locally.

2.4 | Margin concept and planning strategy

In total 117 treatment plans were optimized for the beam models listed in Table 1. The common objective in OPT is a coverage of the target plus margin with the 90% isodose. For each plan, a beam-specific target volume

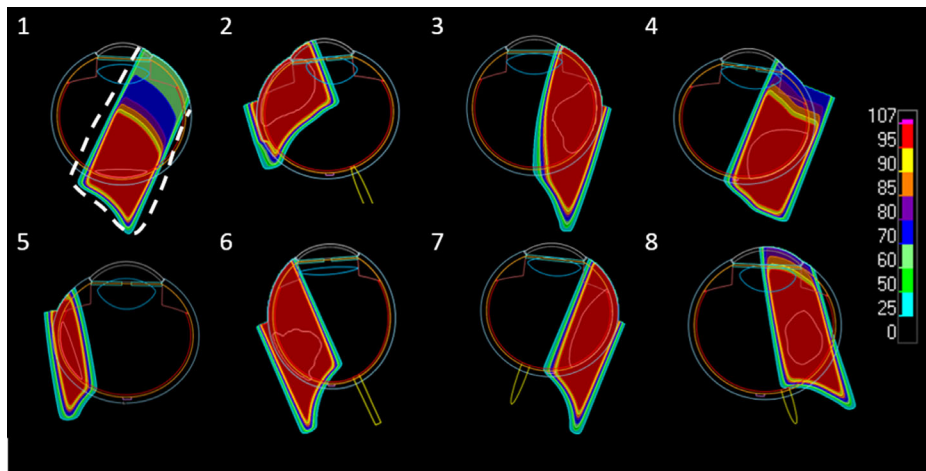


FIGURE 1 Overview of treatment plans (based on beam model distal fall-off (DFO) = 1 mm/lateral penumbra (LP) = 1 mm) for the investigated cases. The light red contour is the delineated target volume. The broken line for case #1 indicates the 50% isodose resulting from model #9. The posterior yellow structure is the optic disc/optic nerve, the magenta colored structure represents the macula in the model

with margins described below was constructed and a conformal coverage with the 90% isodose was realized.

The *lateral aperture margin* to CTV contour was defined depending on the model LP. In order to consider the variable LP of the models, first a constant contribution to lateral margin was deduced from several type B uncertainties as summarized in Table 2, following the concepts of the “Guide to the Expression of Uncertainty in Measurement.”²⁴

The uncertainties were assumed as rectangular probability distributions converted to a standard deviation by applying a coverage factor of $k = 1/\sqrt{3}$ and added in quadrature. This leads to a total systematic and random contribution of 0.24 and 0.29 mm, respectively. Following the van Herk recipe²⁵ a margin of $(2.5 \times 0.24 + 0.7 \times 0.29)$ mm = 0.81 mm results, considering the translational and rotational setup uncertainties as a random contribution, which may persist after online-correction prior treatment. However, given the limited number of fractions all contributions in Table 2 were conservatively considered systematic, leading to a margin of 2.5×0.38 mm = 0.95 mm. RayStation allows the

user to define the lateral aperture margin based on the beams eye view projection for a defined target structure. This needs to consider the above margin and the nominal LP of each model (see Table 1) for a coverage with the 90% isodose. A simple analytical extrapolation, with the LP represented as error-functions, yields $LP(90\%–50\%) = 0.76 \times LP(80\%–20\%)$. A total aperture margin contour was set as 1.7, 2.5, and 4.0 mm for LP = 1, 2, and 4 mm as a starting point.

This margin concept only holds if the LP was constant. Depending on the localization and shape of the target, different depths are associated with different LP due to scatter in tissue. In turn, during manual optimization of the individual treatment plans, slight adjustments of a few tenth of a millimeter were necessary to ensure sufficient coverage at all depths. A manual adjustment was also necessary for plans with a wedge, specifically for the portion of the aperture covered by it. This is due to the increased lateral scatter within the wedge and thus larger LP in this part of the field. In those cases an extra margin of ~ 1 mm was added as a starting point by extending the aperture margin in the beam eye view to the target volume projection below the wedge.²⁶

The *distalproximal* margin was constantly defined as +2.5 mm from CTV as defined in the RayOcular beam parameters. Range and modulation were further adjusted in each plan to ensure a coverage of the beam-specific target volume with the 90% isodose, especially in the case of using wedges. All adjustments were additionally guided by the fundus projection.

TABLE 2 Quantities influencing the lateral margin

Influence quantity	Uncertainty (mm)	Type
Geometric eye model	0.2	Systematic
Clip location within model	0.3	Systematic
Position (translation/rotation)	0.5	Random
Aperture manufacturing	0.1	Systematic
Co-incidence proton versus X-ray	0.2	Systematic

Note: The underlying distribution is considered rectangular for all quantities. The type is either systematic or random, depending on its contribution for a fractionated treatment.

2.5 | Evaluation of plans

The dose distribution of all created treatment plans was analyzed by different dose–volume histogram

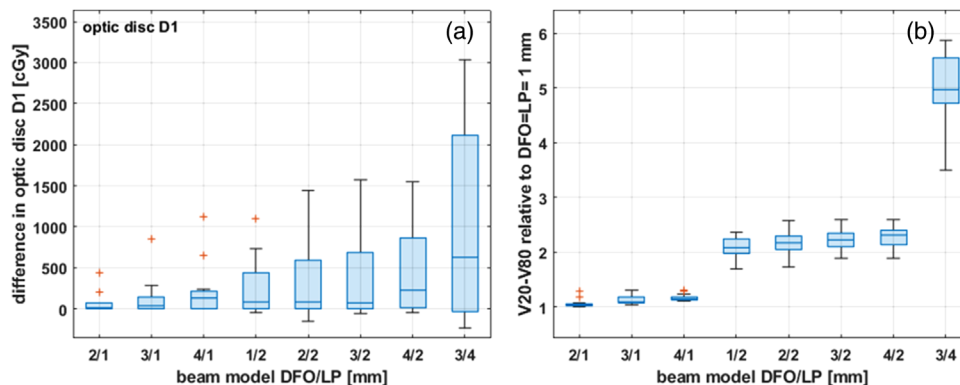


FIGURE 2 (a) Box-Whisker plot showing the distribution of the V20-V80 volume ratios of the plans for each beam model, grouped by distal fall-off (DFO) and lateral penumbra (LP). The underlying results (per case) were calculated as ratio to results for beam model with DFO = LP = 1 mm. (b) Box-chart comparing the different beam models for optic disc D1. All results are given as difference to the results of each plan for model DFO = LP = 1 mm

metrics. Results were calculated as absolute difference or ratio to the reference plan with beam model DFO = LP = 1 mm. Results were extracted from the treatment plans using the RayStation scripting interface and further analyzed in MATLAB R2020a (MathWorks Inc.). The criteria for evaluation were the D1 (dose to 1% of the volume) for macula and optic disc, V30 of optic nerve as well as mean dose Dmean for lens and ciliary body. Historically, the length of the optic nerve is used in EYEPLAN for the evaluation of a treatment plan. RayOcular like OCTOPUS currently does not provide the quantity dose-length histogram though. The V30 (the volume receiving at least 30 Gy(RBE)) was selected as representative for the 50% isodose covering the optic nerve. For instance, with the default model of the optic nerve with 1.5 mm diameter and a length of 10 mm, a V30 = 33% would be equivalent of 3.3 mm length. Additionally the V20-V80 penumbra volume, that is, the difference of volumes encompassed by 20% and 80% of the prescription dose, was calculated.

3 | RESULTS

3.1 | Impact of beam models on plan quality

The DFO and the LP naturally influence the irradiated volume of the eye. This is reflected by the V20-V80 penumbra volume. In Figure 2a, the V20-V80 volume for each beam model is shown as a ratio to the DFO = LP = 1 mm beam model. Figure 2a demonstrates that the V20-V80 penumbra volume is mainly impacted by the LP of the beam model. V20-V80 is more than doubled per millimeter change in LP. The DFO has a considerably smaller impact. The beam model with DFO = 3 mm and LP = 4 mm may result from

a PBS system with aperture, increases the penumbra volume by almost up to a factor of 6 compared to the LP = DFO = 1 mm beam model.

The impact of beam-model parameters for optic disc D1 is shown in Figure 2b, presenting absolute difference to results for beam model DFO = LP = 1 mm. Single plans per beam model (with and without wedge) underlie each box. Some of the plans do not have any relevant dose contribution to optic disc/optic nerve/macula up to a certain DFO/LP and for the same case the wedge plans may be affected more by the changes of LP/DFO than the plans without wedge. The model DFO = 3 mm/LP = 4 mm results in an increase of optic disc D1 by more than 3000 cGy(RBE) for one of the plans.

Figure 3 shows the results for macula D1, optic nerve V30, ciliary body Dmean, and lens Dmean, respectively. The relative reduction in macula D1 for the different beam models is less than for the optic disc (Figure 3a). This can be understood by the fact that in this patient cohort the macula is typically closer to the lateral tumor boundary and may already be exposed to a high-dose level in the plans based on the reference model (DFO = LP = 1 mm). Nevertheless, the general trend of increased dose to the macula can be observed.

The optic nerve volume receiving 30 Gy(RBE) is gradually increasing with increased DFO/LP, with strong dependence on DFO (Figure 3b). The relative increase is much more pronounced than for D1 of the optic disc (Figure 3b). The optic nerve extends from the posterior part of the eye, that is, beyond the distal edge of the dose distribution, where an increase in DFO increases the irradiated volumes. As Figure 3b indicates, the increase in V30 can reach 90%. Together with the aforementioned increase of optic disc D1, such dose levels may result in complete loss of visual capabilities for the treated patient.

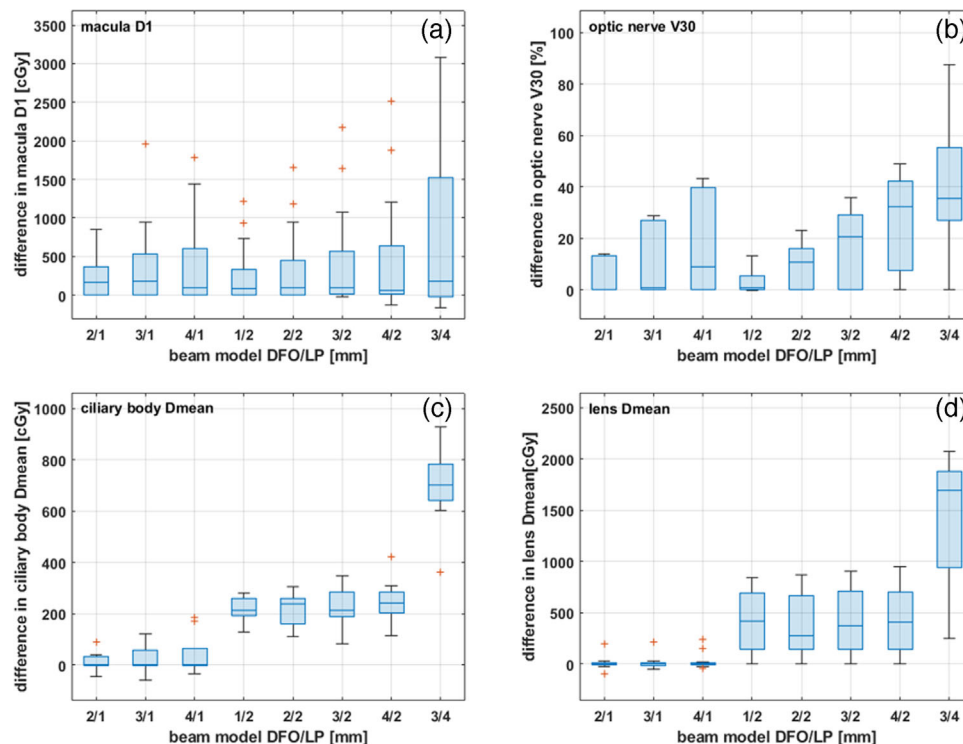


FIGURE 3 F Box–Whisker plots comparing the different beam models for macula D1 (a), V30 for optic nerve (b), mean dose to ciliary body (c), and mean dose to lens (d). All results are given as difference to the results of each plan for model distal fall-off (DFO) = lateral penumbra (LP) = 1 mm

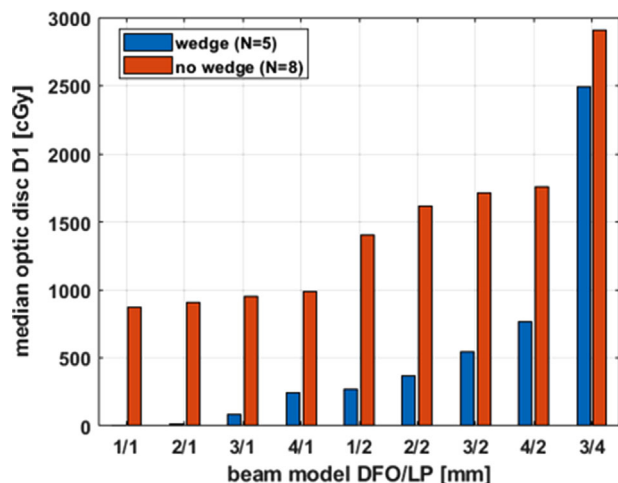


FIGURE 4 Median D1 to optic disc as a function of beam-model parameters in terms of distal fall-off (DFO) and lateral penumbra (LP), either for the five plans with a wedge or the eight plans without

The lens and ciliary body Dmean are more or less only affected by the LP (Figure 3c,d). This can be understood as both OARs are in the proximal region and only one plan (#4) allowed to limit the modulation width to less than the total range.

Figure 4 shows the median optic disc dose D1 for plans with and without a wedge for the different beam models. The wedge offers the possibility for a markedly reduction in dose for the optic disc. Nevertheless, even

for an advanced planning technique employing a wedge, an increased DFO/LP will reduce the plan quality in terms of OAR sparing. On the other hand, the application of a wedge can in some cases compensate for the larger DFO/LP as can be concluded from Figure 4.

4 | DISCUSSION

The results show the expected benefit of a small LP/DFO in sparing OARs in the treatment of uveal melanoma. The volume receiving penumbra dose, that is, dose between 80% and 20%, is naturally affected by the beam LP/DFO. Given rather small volume of the eye this can be considered as an important parameter. The LP showed a larger impact than DFO, except for the irradiated optic nerve volume, which is mainly located at the posterior part of the eye, that is, at the distal end of the dose distribution.

As was shown by the model representing a hypothetical PBS + aperture system (DFO = 3 mm/LP = 4 mm) the quality is always inferior to dedicated single/double-scattering nozzle designs in terms of OAR sparing and irradiated volume outside the target. On the other hand, as recently reported by Ciocca et al.¹¹, the combination of a small energy entering the nozzle and an energy absorber placed far upstream of the collimator, allows to achieve an LP of 1.4–1.7 mm. It needs to be noted that the flexibility which is offered by PBS in terms of dose

modulation is limited due to the large underlying single spot sizes of such a system ranging between 1.6 and 6 cm full-width half maximum (see Refs.^{11,21,27}). In order to take an advantage of the PBS technique for explicit sparing of OARs, variable collimator systems would be required such as described by Hyer et al.²⁸ Such a concept on the target size scale for uveal melanoma is however not yet clinically available.

The fact that the penumbra volume is more sensitive to LP than DFO can be explained by the fact that the average modulation width of all plans is ~ 19 mm with an average range of ~ 20 mm. That means for most plans the proximal dose is 100% and not affected by any change in DFO. The larger impact of LP than DFO with respect to the “penumbra volume” V20–V80 can also be understood by a simple geometric consideration of a cylinder’s surface. If the dose volume covering the target is approximated as a cylinder, the LP must have a larger contribution than the DFO to a change in cylinder’s surface S . The partial derivative of a cylinder’s surface equation with radius r and height h results in $dS = dh \times 2\pi r + dr \times 2\pi(h + 2r)$. For example, the surface change for a cylinder with $h = 20$ mm and $r = 7$ mm is factor 4.8 larger for $dr = 1$ mm than for $dh = 1$ mm.

For posterior tumors a small DFO helps to reduce dose to macula, optic disc, and optic nerve (see, e.g., Figure 4). This may be important for conservation of vision by maintaining the high standard of tumor control in ocular PT.^{18,29,30}

In all cases the gaze angle was kept constant and taken from the original clinical plans. Thus, the gaze angle may have been further optimized when considering the dose distribution of each model.³¹ The number of patient plans investigated was limited, but considered representing typical cases found in ocular PT. The patient mix that is treated by a facility certainly impacts the findings.

In the present study, a margin only considered setup and machine uncertainties from a CTV while institutions may incorporate microscopic extension, etc., in the lateral margins and thus other aperture margins may result clinically. However, the resulting aperture margin based on the selected uncertainties (Section 2.4) are comparable to a universally applied 2.5 mm aperture margin.^{4,6,8,14–17} Thus, the treatment plans analyzed are considered as representable for clinical dose distributions that would result from the employed beam models. The result of the required margins and thus dose to OARs strongly depends on the interpretation of the involved uncertainties and each OPT center may have a different understanding on each contribution. For example, the underlying probability distribution of each delivery uncertainty may be interpreted as rectangular as was done in the present study (see Section 2.4) but could also be interpreted as a normal distribution with direct impact on the margins.

The application of a wedge generally shows superior dose distribution in terms of OAR sparing. The application of a wedge can in some cases compensate for the larger DFO/LP, that is, in terms of OAR dose plans with a wedge may be comparable to a plan without a wedge but smaller DFO/LP.

The dose calculation in the employed TPS RayOcular is based on a pencil-beam algorithm. This is in contrast to, for example EYEPLAN, where a simple look-up table serves as algorithm. Given the small field sizes, a validation of the RayOcular approach is warranted, but a detailed investigation of the pencil-beam algorithm accuracy is beyond the scope of this work. As the present study directly compared different LP/DFO values, the accuracy itself is not expected to directly impact the conclusions drawn.

5 | CONCLUSION

The planning study with the RayOcular TPS demonstrates the impact of beam properties in terms of LP and DFO for proton treatment of uveal melanoma. The LP shows to be of greater importance than the DFO. The findings reported in this study suggest that a proper collimation design is a prerequisite for a clinical shift toward PBS integrating an aperture system. DFO is more important in posterior tumors than in anterior locations, which is caused by locations of OARs in the posterior parts of the eye. Without limiting indications, it is thus may be required to limit the energy entering an eye treatment nozzle.

The application of a wedge is generally beneficial in all cases and should be considered when a sparing of optic disc/nerve and macula is limited for systems with large DFO/LP. Accurate modeling of the changes in the dose distribution due to a wedge in a TPS is however crucial. A thorough validation of RayOcular for modeling wedges is currently being prepared.

In general, it should be the goal for future PBS-based solutions to achieve the quality of dedicated nozzle designs for ocular PT to maintain the existing high quality in ocular PT.

ACKNOWLEDGEMENTS

The authors would like to thank D. Cordini, R. Stark and A. Weber of HZB for their valuable input to 3D treatment planning in ocular proton therapy. H. Siregar (WPE) is acknowledged for her comments on the manuscript.

Open access funding enabled and organized by Projekt DEAL.

FUNDING INFORMATION

None.

CONFLICT OF INTERESTS

Martin Janson is an employee of RaySearch Laboratories (Stockholm, Sweden), the company that has developed and is selling the treatment planning system RayStation that was used for this study. The other authors do not have any conflict of interest.

REFERENCES

- Goitein M, Miller T. Planning proton therapy of the eye. *Med Phys*. 1983;10(3):275-283.
- Hrbacek J, Mishra KK, Kacperek A, et al. Practice patterns analysis of ocular proton therapy centers: the international OPTIC survey. *Int J Radiat Oncol Biol Phys*. 2016;95(1):336-343.
- van Beek JGM, Ramdas WD, Angi M, et al. Local tumour control and radiation side effects for fractionated stereotactic photon beam radiotherapy compared to proton beam radiotherapy in uveal melanoma. *Radiother Oncol*. 2021;157:219-224.
- Egger E, Schalenbourg A, Zografos L, et al. Maximizing local tumor control and survival after proton beam radiotherapy of uveal melanoma. *Int J Radiat Oncol Biol Phys*. 2001;51(1):138-147.
- Seibel I, Cordini D, Rehak M, et al. Local recurrence after primary proton beam therapy in uveal melanoma: risk factors, retreatment approaches, and outcome. *Am J Ophthalmol*. 2015;160(4):628-636.
- Slopsema RL, Mamalui M, Zhao T, Yeung D, Malyapa R, Li Z. Dosimetric properties of a proton beamline dedicated to the treatment of ocular disease. *Med Phys*. 2014;41(1):011707.
- Fleury E, Trnková P, Spruijt K, et al. Characterization of the HollandPTC proton therapy beamline dedicated to uveal melanoma treatment and an interinstitutional comparison. *Med Phys*. 2021;48(8):4506-4522.
- Kacperek A. Ocular proton therapy centers. In: Linz U, editor. *Ion Beam Therapy – Fundamentals, Technology, Clinical Applications*. Berlin, Heidelberg: Springer-Verlag; 2012:149-177.
- Bäumer C, Janson M, Timmermann B, Wulff J. Collimated proton pencil-beam scanning for superficial targets: impact of the order of range shifter and aperture. *Phys Med Biol*. 2018;63(8):085020.
- Bäumer C, Plaude S, Khalil DA. Clinical implementation of proton therapy using pencil-beam scanning delivery combined with static apertures. *Front Oncol*. 2021;11:599018.
- Ciocca M, Magro G, Mastella E. Design and commissioning of the non-dedicated scanning proton beamline for ocular treatment at the synchrotron-based CNAO facility. *Med Phys*. 2019;46(4):1852-1862.
- Heufelder J, Cordini D, Fuchs H, et al. Fünf Jahre protonentherapie von Augentumoren am Hahn-Meitner-Institut Berlin. *Z Med Phys*. 2004;14(1):64-71.
- Weber DC, Bogner J, Verwey J, et al. Proton beam radiotherapy versus fractionated stereotactic radiotherapy for uveal melanomas: a comparative study. *Int J Radiat Oncol Biol Phys*. 2005;63(2):373-384.
- Damato B, Kacperek A, Chopra M, Campbell IR, Errington RD. Proton beam radiotherapy of choroidal melanoma: the Liverpool-Clatterbridge experience. *Int J Radiat Oncol Biol Phys*. 2005;62(5):1405-1411.
- Dendale R, Lumbroso-Le Rouic L, Noel G, et al. Proton beam radiotherapy for uveal melanoma: results of Curie Institut-Orsay proton therapy center (ICPO). *Int J Radiat Oncol Biol Phys*. 2006;65(3):780-787.
- Mishra KK, Daftari IK. Proton therapy for the management of uveal melanoma and other ocular tumors. *Chin Clin Oncol*. 2016;5(4):50.
- Sas-Korczyńska B, Markiewicz A, Romanowska-Dixon B, Pluta E. Preliminary results of proton radiotherapy for choroidal melanoma – the Kraków experience. *Contemp Oncol (Pozn)*. 2014;18(5):359-366.
- Thariat J, Grange JD, Mosci C, et al. Visual outcomes of parapapillary uveal melanomas following proton beam therapy. *Int J Radiat Oncol Biol Phys*. 2016;95(1):328-335.
- Daftari IK, Mishra KK, O'Brien JM, et al. Fundus image fusion in EYEPLAN software: an evaluation of a novel technique for ocular melanoma radiation treatment planning. *Med Phys*. 2010;37(10):5199-5207.
- Dobler B, Bendl R. Precise modelling of the eye for proton therapy of intra-ocular tumours. *Phys Med Biol*. 2002;47(4):593-613.
- Winterhalter C, Lomax A, Oxley D, Weber DC, Safai S. A study of lateral fall-off (penumbra) optimisation for pencil beam scanning (PBS) proton therapy. *Phys Med Biol*. 2018;63(2):025022.
- Maes D, Regmi R, Taddei P, et al. Parametric characterization of penumbra reduction for aperture-collimated pencil beam scanning (PBS) proton therapy. *Biomed Phys Eng Express*. 2019;5(3):035002.
- International Commission on Radiation Units and Measurements. *ICRU Report 78 – prescribing, recording, and reporting proton-beam therapy*. J ICRU. 2007;7. Oxford University Press.
- Evaluation of Measurement Data — Guide to the Expression of Uncertainty in Measurement. *Joint Committee for Guides in Metrology*; 2008.
- van Herk M. Errors and margins in radiotherapy. *Semin Radiat Oncol*. 2004;14(1):52-64.
- Rethfeldt C, Fuchs H, Gardey KU. Dose distributions of a proton beam for eye tumor therapy: hybrid pencil-beam ray-tracing calculations. *Med Phys*. 2006;33(3):782-791.
- Bäumer C, Fuentes C, Janson M, Matic A, Timmermann B, Wulff J. Stereotactical fields applied in proton spot scanning mode with range shifter and collimating aperture. *Phys Med Biol*. 2019;64(15):155003.
- Hyer DE, Hill PM, Wang D, Smith BR, Flynn RT. A dynamic collimation system for penumbra reduction in spot-scanning proton therapy: proof of concept. *Med Phys*. 2014;41(9):091701.
- Riechardt AI, Stroux A, Seibel I, et al. Side effects of proton beam therapy of choroidal melanoma in dependence of the dose to the optic disc and the irradiated length of the optic nerve. *Graefes Arch Clin Exp Ophthalmol*. 2020;258(11):2523-2533.
- Pica A, Weber DC, Vallat L, et al. Good long-term visual outcomes of parapapillary choroidal melanoma patients treated with proton therapy: a comparative study. *Int Ophthalmol*. 2021;41(2):441-452.
- Hennings F, Hennings F, Lomax A, Pica A, Weber DC, Hrbacek J. Automated treatment planning system for uveal melanomas treated with proton therapy: a proof-of-concept analysis. *Int J Radiat Oncol Biol Phys*. 2018;101(3):724-731.

How to cite this article: Wulff J, Koska B, Janson M, et al. Impact of beam properties for uveal melanoma proton therapy—An in silico planning study. *Med Phys*. 2022;49 3481–3488. <https://doi.org/10.1002/mp.15573>